J. Geogr. Sci. 2014, 24(1): 3-17
DOI: 10.1007/s11442-014-1069-3

Modeling net primary productivity of the terrestrial ecosystem in China from 1961 to 2005

YUAN Quanzhi[1], *WU Shaohong[2], ZHAO Dongsheng[2], DAI Erfu[2], CHEN Li[2], ZHANG Lei[1]

1. Institute of Remote Sensing and Digital Earth, CAS, Beijing 100101, China;
2. Institute of Geographic Sciences and Natural Resources Research, CAS, Beijing 100101, China

Abstract: Net primary productivity (NPP) is the most important index that represents the structure and function of the ecosystem. NPP can be simulated by dynamic global vegetation models (DGVM), which are designed to represent vegetation dynamics relative to environmental change. This study simulated the NPP of China's ecosystems based on the DGVM Integrated Biosphere Simulator (IBIS) with data on climate, soil, and topography. The applicability of IBIS in the NPP simulation of China's terrestrial ecosystems was verified first. Comparison with other relevant studies indicates that the range and mean value of simulations are generally within the limits of observations; the overall pattern and total annual NPP are close to the simulations conducted with other models. The simulations are also close to the NPP estimations based on remote sensing. Validation proved that IBIS can be utilized in the large-scale simulation of NPP in China's natural ecosystem. We then simulated NPP with climate change data from 1961 to 2005, when warming was particularly striking. The following are the results of the simulation. (1) Total NPP varied from 3.61 GtC/yr to 4.24 GtC/yr in the past 45 years and exhibited minimal significant linear increase or decrease. (2) Regional differences in the increase or decrease in NPP were large but exhibited an insignificant overall linear trend. NPP declined in most parts of eastern and central China, especially in the Loess Plateau. (3) Similar to the fluctuation law of annual NPP, seasonal NPP also displayed an insignificant increase or decrease; the trend line was within the general level. (4) The regional differences in seasonal NPP changes were large. NPP declined in spring, summer, and autumn in the Loess Plateau but increased in most parts of the Tibetan Plateau.

Keywords: net primary productivity; integrated biosphere simulator; China

1 Introduction

Net primary productivity (NPP) is the accumulated organic matter produced by green plants in a unit area and unit time; it is the amount of residue gained after photosynthesis, deducting that consumed by autotrophic respiration (Lieth *et al*., 1975). NPP is not only a direct

---

Received: 2013-02-01 **Accepted:** 2013-06-28
Foundation: "Strategic Priority Research Program of China" of the Chinese Academy of Sciences, No.XDA05090307; National Key Technology R&D Program of the 12th Five-Year Plan, No.2012BAC19B10; Open Project of Shanghai Key Lab for Urban Ecological Processes and Eco-Restoration, No.SHUES2012A04
Author: Yuan Quanzhi, PhD, specialized in simulations of land surface processes. E-mail: yqz_108@163.com
***Corresponding author:** Wu Shaohong, Professor, specialized in physical geography. E-mail: wush@igsnrr.ac.cn

reflection of the production capacity and quality of the ecosystem but is also a major factor that determines the carbon source or carbon sink of the ecosystem, thus playing an important role in the global carbon cycle (Ruimy *et al*., 1994; Field *et al*., 1998; Wang *et al*., 2002).

NPP in natural vegetation is mainly dominated by climatic conditions apart from the biological characteristics of the soil and vegetation itself. NPP can be estimated by establishing a mathematical model to simulate the interactions between the biosphere and atmosphere. However, some of the models utilized to estimate NPP focus only on a limited range of ecosystem processes depending on their purpose, including terrestrial biogeochemistry processes (Parton *et al*., 1993; Potter *et al*., 1993), and biogeography processes (Prentice *et al*., 1992). Several models that link land surface, terrestrial biogeochemical processes, and equilibrium vegetation cover were designed to improve understanding of the interactions between the biosphere and atmosphere (Sellers *et al*., 1992; Haxeltine and Prentice, 1996). Another limitation of these models is that they mainly consider the equilibrium relationship between the atmosphere and biosphere and do not describe the dynamic interactions that occur within the terrestrial biosphere. Dynamic global vegetation models (DGVMs) were designed recently to represent vegetation dynamics relative to environmental change and to better understand terrestrial biosphere processes and their potential response to climate change (Foley *et al*., 1996; Friend *et al*., 1997; Sitch *et al*., 2000).

Integrated Biosphere Simulator (IBIS) as a DGVM can dynamically simulate the transient interactions between vegetation and atmosphere. IBIS is a comprehensive model of the terrestrial biosphere (Foley *et al*., 1996; Kucharik *et al*., 2000). This model involves the integration of land surface, biophysical and biogeochemical processes such as plant physiology and nutrient cycling, and vegetation dynamics. Since its establishment, IBIS has been validated, modified, and applied in many studies from site scale to global scale (Delire and Foley, 1999; El Maayar *et al*., 2001, 2002; Naik *et al*., 2003; Twine *et al*., 2004; Liu *et al*., 2005; Kucharik *et al*., 2006; Vano *et al*., 2006; Zheng and Wang, 2007; Zhu *et al*., 2010). IBIS can be utilized in the large-scale simulation of the potential terrestrial natural vegetation map of China through parameter adjustments (Yuan *et al*., 2011).

Since the industrial revolution, greenhouses gases (such as CO_2, CH_4, and N_2O) produced from human activities and released into the atmosphere have significantly altered the chemical components of the atmosphere, leading to dramatic changes in the global climate (IPCC, 2007). China's annual average temperature increased by 0.5℃ to 0.8℃ over the past century; annual average temperature was slightly higher than the global average during the same period, and warming was particularly striking for nearly 50 years (Ding *et al*., 2006). Drastic climate change has a huge impact on terrestrial ecosystems, generating possible changes in the structure, composition, and biomass of the vegetation community (Foley *et al*., 1998; Matthew *et al*., 2000; Parry *et al*., 2007; Wu *et al*., 2010). China's terrestrial ecosystems with their vulnerable ecological environments are very sensitive to climate change. Therefore, understanding the relationship between terrestrial ecosystems and climate change as well as analyzing the dynamic response of terrestrial ecosystems to climate change in China has attracted significant attention (Tao *et al*., 2003; Gao *et al*., 2004; Fu *et al*., 2005; Wu *et al*., 2007).

IBIS was further validated in this study prior to its application in the simulation of China's terrestrial NPP. The dynamic changes in China's terrestrial ecosystems in the past

45 years (1961 to 2005) were simulated for the analysis of corresponding temporal and spatial variations in NPP.

2 Data and model

2.1 Input data

IBIS was utilized with climate, soil, and topography data input at 0.5° × 0.5° spatial resolution. Climate data were interpolated with ANUSPLIN based on observations obtained from 756 meteorological stations from 1961 to 2005 (Figure 1). Climate data included monthly mean air temperature, precipitation, relative humidity, cloudiness, diurnal temperature range, wind speed, and number of wet days. Soil data were obtained from the Center for Sustainability and the Global Environment. Data on topography were a resample of DEM with an original resolution of 30″.

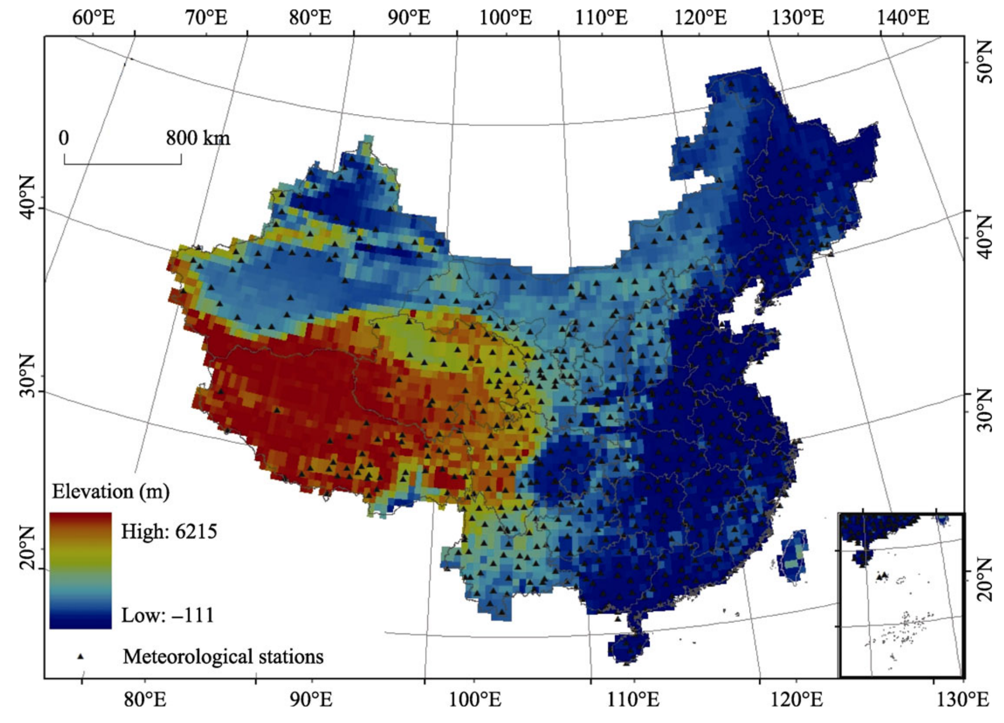

Figure 1 Geographic distribution of the 756 meteorological stations and DEM with a resolution of 0.5° × 0.5°

We calculated the coefficients of determination (R^2) between the observed and simulated monthly values to evaluate the performance of interpolations. The simulated monthly mean air temperature, precipitation, relative humidity, cloudiness, diurnal temperature range, number of wet days, and wind speed fit the observations reasonably with average R^2 greater than 0.9 (R^2 of wind speed was 0.8).

2.2 Model description

IBIS organizes land surface processes, underground carbon and nitrogen cycling, vegetation phenology, and vegetation dynamics within a hierarchical framework. The land surface module, which involves two layers of vegetation and six layers of soil, represents surface energy cycling and material balance. The underground carbon and nitrogen cycling module links the growth of microbial biomass and litter pools derived from leaf turnover, woody detritus, and fine root turnover. The vegetation phenology module describes the deciduous behavior of plant functional types (PFTs) in relation to climatic conditions through an empirical formula. The vegetation dynamic module simulates the time-dependent interactions between vegetation and climate change. IBIS employs a set of climate constraints such as growing degree–day (GDD) requirement, cold tolerance limits, and minimum chilling requirements to determine the range of existence of PFTs. The different PFTs (e.g., temperate broadleaf deciduous trees, deciduous shrubs, and cool grasses) in each grid cell compete for light and water according to their abilities (characterized in Table 1) (Foley *et al*., 1996; Kucharik *et al*., 2000; Yuan *et al*., 2011).

3 Results

3.1 Model validation

We simulated the terrestrial NPP of China from 1961 to 2005 at average climatic conditions. The results were then compared with observations in other studies, simulations conducted with other vegetation models, and estimations based on remote sensing to verify the simulation.

3.1.1 Comparison with observations in other studies

Comparison of the simulated terrestrial NPP with observations in other studies (Table 2) indicates that the range and mean value of the simulated NPP are generally within the limits of the observations (Lieth *et al*., 1975; Liu *et al*., 1993; Wang *et al*., 2001; Liu *et al*., 1994).

3.1.2 Comparison with simulations conducted with other models

Simulations of China's terrestrial NPP have been performed extensively in recent years. We compared the annual terrestrial NPP simulated by IBIS with that in other relevant studies (Table 3). Results show that the IBIS simulation is close to the results obtained by Xiao *et al*. (1998), Sun *et al*. (2001), Cao *et al*. (2003), Huang (2005) and Zhao (2009).

3.1.3 Comparison with estimations based on remote sensing

The simulated NPP presented in this paper is NPP of the natural ecosystem based on natural environment data, including climate, topography, and soil data. We selected the NPP of 30 national nature reserves (Figure 2) to conduct the simulation because these reserves are less directly affected by human activities. We utilized estimated NPP based on remote sensing data to verify the simulation results. The estimations, calculated by the GLO–PEM model, came from the Resources and Environment Science Data Center of Chinese Academy of Sciences.

Figure 3 presents the R^2 of simulations and estimations from 1981 to 2000 for the 30 selected points. The IBIS simulation results are generally close to the estimations based on remote sensing.

In summary, the IBIS simulations are generally within the limits of the observations, similar to other simulations of total annual terrestrial NPP and overall pattern, and generally

Table 1 Definition of each PFT in IBIS after parameter adjustment

Trees	m	b	$V_{m,15}$	T_{min} (℃)	T_{min} (℃)	GDD_5	σ, m^{2}kg^{-1}	α_{leaf}	α_{root}	α_{stem}	τ_{leaf} years	τ_{root} years	τ_{stem} years
Tropical broadleaf evergreen	10.0	0.01	65.0	>5.0			25.0	0.30	0.20	0.50	1.01	1.0	25.0
Tropical broadleaf drought-deciduous	10.0	0.01	65.0	>5.0			25.5	0.30	0.20	0.50	1.00	1.0	25.0
Subtropical broadleaf evergreen	10.0	0.01	40.0	>–10.0	<5.0		25.0	0.30	0.20	0.50	1.00	1.0	25.0
Temperate conifer evergreen	6.0	0.01	30.0	>–45.0	<–10.0	>1200	12.5	0.30	0.40	0.30	2.00	1.0	50.0
Temperate broadleaf cold-deciduous	10.0	0.01	30.0	>–45.0	<–10.0	>1200	25.0	0.30	0.20	0.50	1.00	1.0	50.0
Boreal conifer evergreen	6.0	0.01	25.0	>–57.5	<–45.0	>350	12.5	0.30	0.40	0.30	2.50	1.0	100.0
Boreal broadleaf cold-deciduous	10.0	0.01	30.0	>–57.5	<–45.0	>350	25.0	0.30	0.20	0.50	1.00	1.0	100.0
Boreal conifer cold-deciduous	6.0	0.01	30.0		<–45.0	>350	25.1	0.30	0.20	0.50	1.00	1.0	100.0
Shrubs and Grasses	m	b	$V_{m,15}$	T_w (℃)		GDD_0	σ,m^{2}kg^{-1}	α_{leaf}	α_{root}	α_{stem}	τ_{leaf} years	τ_{root} years	τ_{stem} years
Evergreen shrubs	9.0	0.01	6.0			>100	12.5	0.45	0.40	0.15	1.50	1.0	5.0
Cold-deciduous shrubs	9.0	0.01	27.5			>100	25.0	0.45	0.35	0.20	1.00	1.0	5.0
Warm (C4) grasses	4.0	0.04	4.0	>22.0		>100	20.0	0.45	0.55	0.00	1.25	1.0	n/a
Cool (C3) grasses	9.0	0.01	25.0			>100	20.0	0.45	0.55	0.00	1.00	1.0	n/a

Original definition of the PFTs in IBIS follows Kucharik *et al.* (2000). Yuan *et al.* (2011) adjusts a part of the climatic constraints and physiological parameters of PFTs.
M, the slope of the stomatal conductance relationship (nondimensional); b, intercept of the stomatal conductance relationship (mol H_2O m^{-2} s^{-1}); $V_{m,15}$, at 15ßC maximum Rubisco capacity of the top leaf (μmol CO_2 m^{-2} s^{-1}); T_{min}, absolute minimum temperature; T_w, temperature of the warmest month; GDD_0, growing degree days calculated on a 0ßC base; GDD_5, growing degree days calculated on a 5ßC base, σ, specific leaf area; α, allocation fraction of total photosynthate; τ, residence time of carbon.

Table 2 Comparison of simulated and measured NPP (gC/m^2/yr)

Type of ecological system	Observations	Simulated NPP during 1961–2005		
		Vegetation type	Range	Mean
Evergreen broadleaf forest	600–3500	Tropical evergreen forest	1024.1–1604.2	1243.0
		Subtropical evergreen broadleaf forest	132.1–1250.8	1072.1
Evergreen conifer forest	160–1500	Temperate evergreen conifer forest	601.1–725.3	678.7
		Boreal evergreen forest	78.8–578.3	408.3
Deciduous broadleaf forest	250–2500	Deciduous broadleaf forest	271.7–804.8	501.5
Deciduous conifer forest	150–1621	Boreal deciduous conifer forest	105.2–533.7	359.9
Mixed forest	250–2500	Mixed forest	323.1–761.9	582.7
Scrubland	4–1200	Dense scrubland	203.9–214.2	214.0
		Open scrubland	61.5–89.5	75.4
Open forest	200–2000	Open forest	226.9–355.3	278.2
Grassland	100–727	Grassland	88.5–358.2	203.6
Tundra	90–400	Tundra	10.2–437.5	165.0
Desert	0–250	Desert	0–64.1	9.8
		Polar desert	0–10.3	3.0

Table 3 Comparison with simulation results of other models

Period	Model	Spatial resolution	NPP (Pg C yr^{-1})	References
	TEM	0.5°	3.65	Xiao *et al*., 1998
1992	Miami	1km	3.72	Sun *et al*., 1999
1981–2000	CEVSA	0.1°	3.27	Cao *et al*., 2003
1981–2000	AVIM2	0.1°	3.44	Huang, 2005
1961–1990	LPJ	0.5°	3.86	Zhao, 2010
1961–2005	IBIS	0.5°	3.87	This study

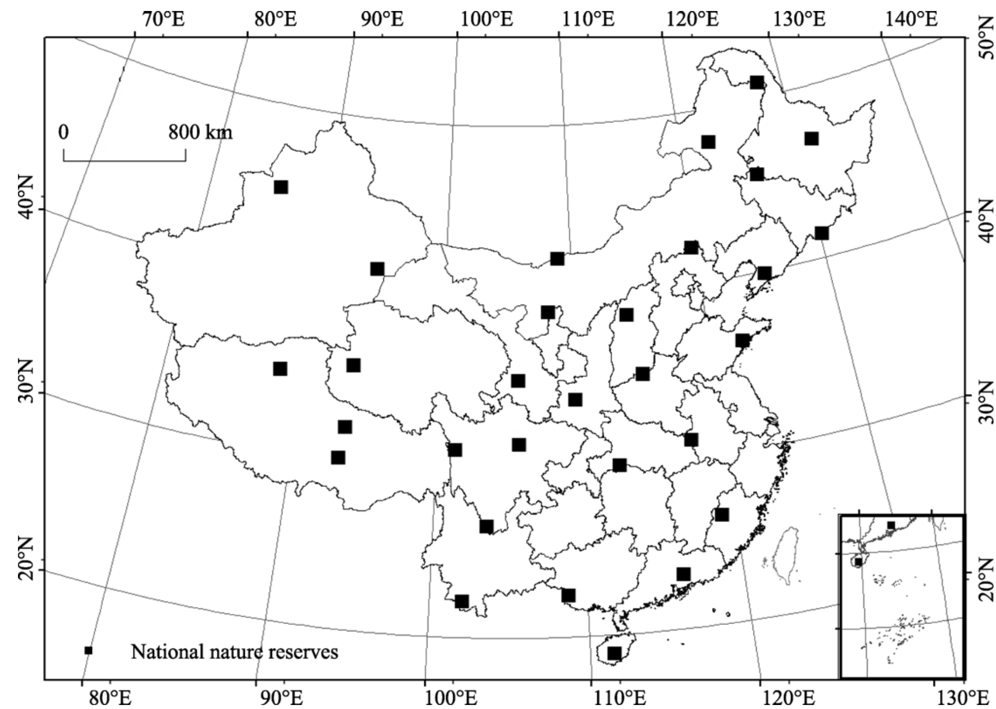

Figure 2 Distribution of the 30 selected national nature reserves

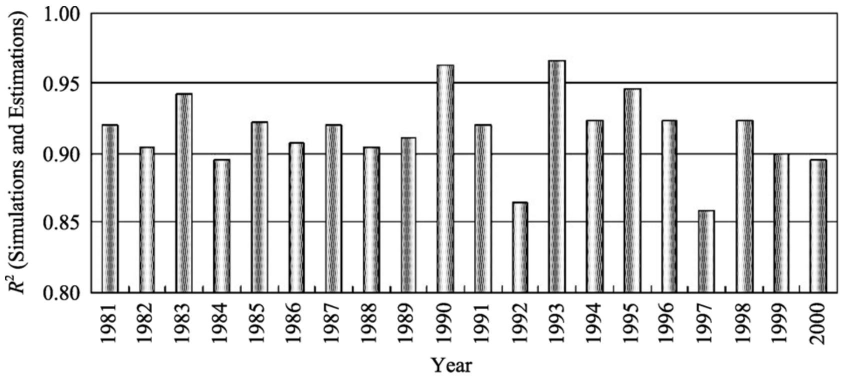

Figure 3 Fit tests for the simulations and estimations based on remote sensing

close to the NPP estimations of 30 national nature reserves. IBIS is therefore suitable for the simulation of terrestrial NPP in China.

3.2 Spatial distribution of NPP

The simulated annual NPP demonstrated a trend of progressive decrease from the southeast coast to the northwest inland. Ecosystems in the southern, central, and southwestern parts had the highest NPP; the NPP of ecosystems in the northeastern, eastern and northern parts, Inner Mongolia, and eastern and central Tibetan Plateau followed, respectively. The lowest NPP value was simulated in the northwestern and western parts of the Tibetan Plateau (Figure 4).

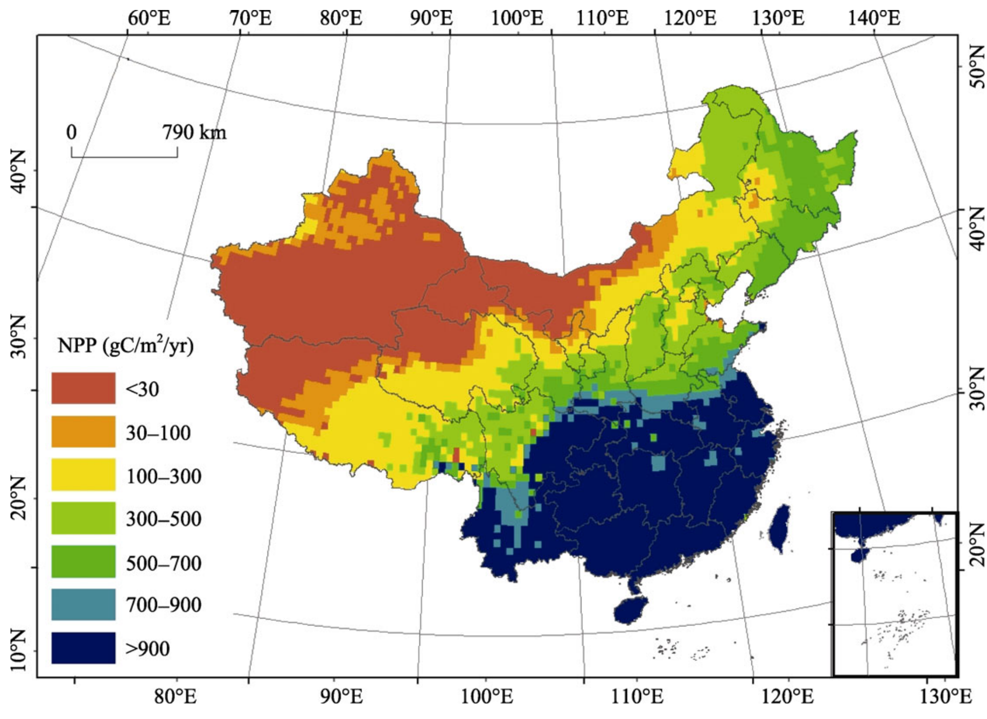

Figure 4 IBIS-simulated spatial distribution of terrestrial NPP in China

We selected four profiles along the coordinates 110°E, 115°E, 30°N, and 40°N to analyze the longitudinal and latitudinal distribution features of China's terrestrial NPP (Figure 5). Along the 30°N profile, NPP increased gradually with a significant increase from 300 gC/m^2/yr to 1000 gC/m^2/yr near 103°N where the transitional region from Tibetan Plateau to Sichuan Basin is located. NPP along the 40°N profile was almost between 79°E to 107°E in the desert areas and then increased gradually in grassland and temperate forests. The 110°E profile between 19°N to 21°N passed through tropical forests; NPP was generally higher than 1100 gC/m^2/yr. NPP declined slightly toward the north when the profile passed through subtropical forests until 32°N and then rapidly decreased in temperate forests, grasslands, and deserts. Similarly, NPP along 115°E was between 900 gC/m^2/yr to 1100 gC/m^2/yr when the profile crossed subtropical forests and then declined as it went through forests and grasslands in a temperate area.

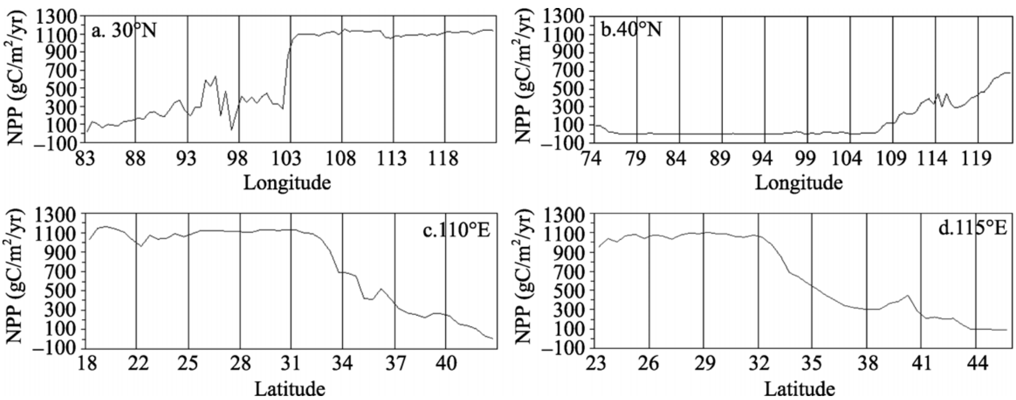

Figure 5 Longitudinal and latitudinal profiles of NPP

3.3 Annual total NPP variability

3.3.1 Inter-annual variability of NPP

Simulation results show that China's total annual NPP ranged from 3.60 GtC to 4.25 GtC from 1961 to 2005 (Figure 6), with an average value of 3.87 GtC/yr, standard deviation of 0.136 GtC/yr, and a coefficient of variation (CV) of 3.53%. The maximum value was observed in 1990, and the minimum value was observed in 1966 and 2001. Overall, the total annual NPP did not present a significant increase or decrease; the linear slope of the trend line was –0.0006.

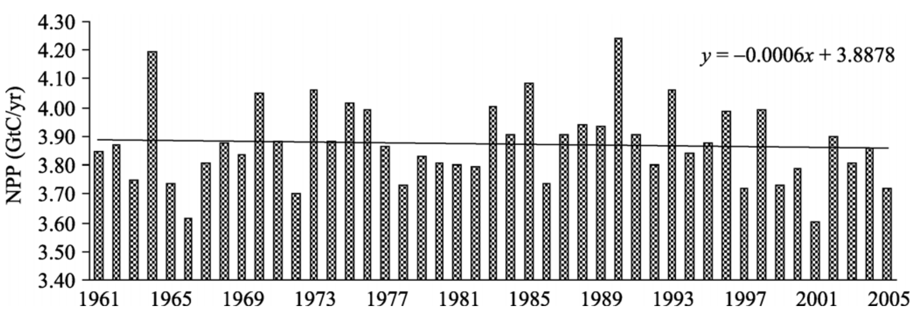

Figure 6 Simulated annual NPP of Chinese terrestrial ecosystems from 1961 and 2005

3.3.2 Seasonal variability of NPP

Studies on the seasonal variability of NPP improve our understanding of the interrelation between climatic systems and terrestrial ecosystems (Ni, 2000; Piao and Fang, 2003). Summer provided the largest contribution to NPP with an average of 1.56 GtC/quarter, accounting for 40.2% of total NPP, followed by autumn with 1.03 GtC/quarter, accounting for 26.7%, and spring with 0.91 GtC/quarter, accounting for 23.5%. NPP was the lowest in winter, with an average of 0.37 GtC/quarter, accounting for merely 9.7%. Fluctuation in NPP at all seasons did not exhibit a significant increase or decrease, and the trend line was within the general level (Figure 7). Among the seasons, autumn exhibited the largest NPP decrease with an annual decrease of 0.0011 GtC. Annual NPP increased in spring and summer with a linear slope of 0.0001 and 0.0003, respectively. NPP in winter showed a small decrease of 0.00005 GtC/year probably because of the lack of vegetation growth in most areas in northern China.

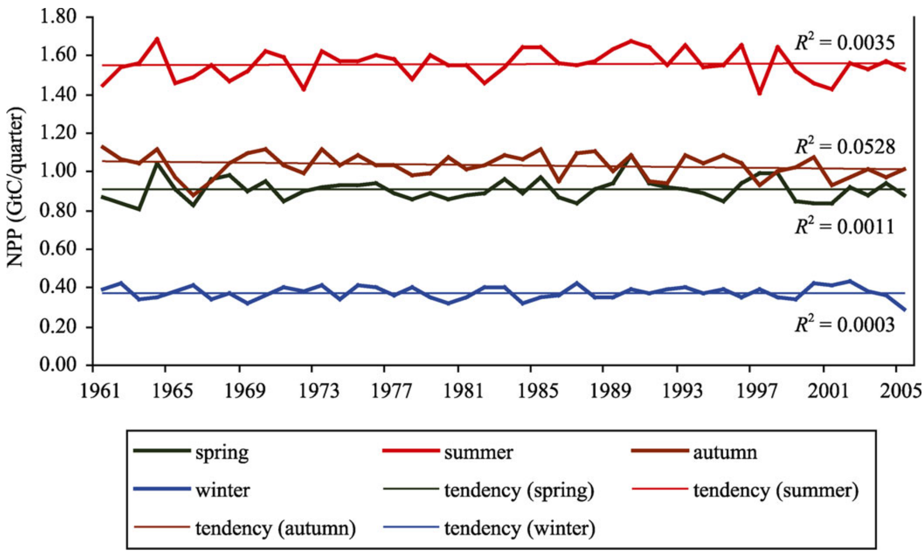

Figure 7 Seasonal variability of Chinese terrestrial NPP from 1961 to 2005

3.4 Regional NPP variability

NPP variation in every latitude–longitude grid as a result of climate change over the past 45 years (1961 to 2005) was collected and analyzed, leading to the conclusions discussed below.

3.4.1 Regional NPP inter-annual variability

We examined NPP and the years of all latitude–longitude grids through unitary linear regression analysis. The respective annual linear trend of NPP and the corresponding determination coefficients (R^2) are presented in Figure 8.

The figure shows that regional differences in the increase or decrease of NPP were significant from 1961 to 2005 but presented an insignificant linear trend. NPP declined in most parts of eastern China. A large average annual decline in NPP was observed in the

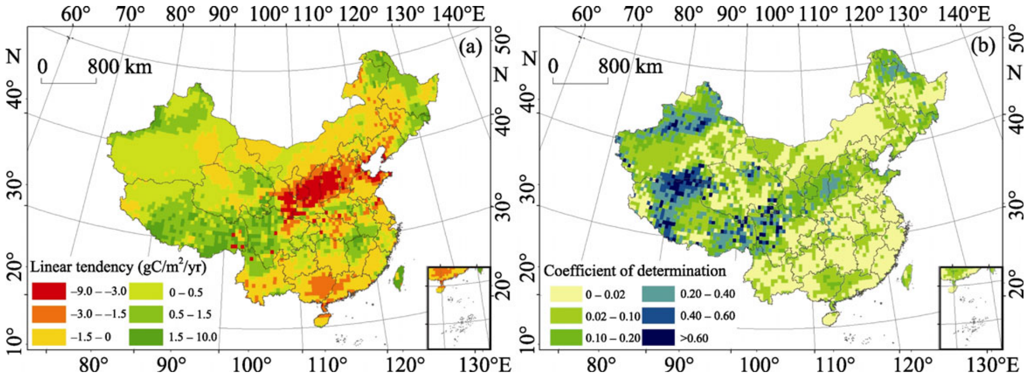

Figure 8 Linear trend and determination coefficient (R^2) of annual NPP from 1961–2005

Loess Plateau, with NPP decreasing by more than 3.0 gC/m^2/yr in most areas. NPP increased slightly in most parts of western China. However, NPP increased dramatically in the central–eastern parts of the Tibetan Plateau and northern part of the Greater Hinggan Mountains. The linear increase in NPP in the Kunlun Mountain area was significant, which proves that favorable development occurred in the natural ecosystem of this region during the 45-year period of climate change.

3.4.2 Regional seasonal changes in NPP

Figure 9 presents the variation in regional NPP in all seasons from 1961 to 2005. NPP in most parts of the Loess Plateau decreased sharply in spring, summer, and autumn, generally

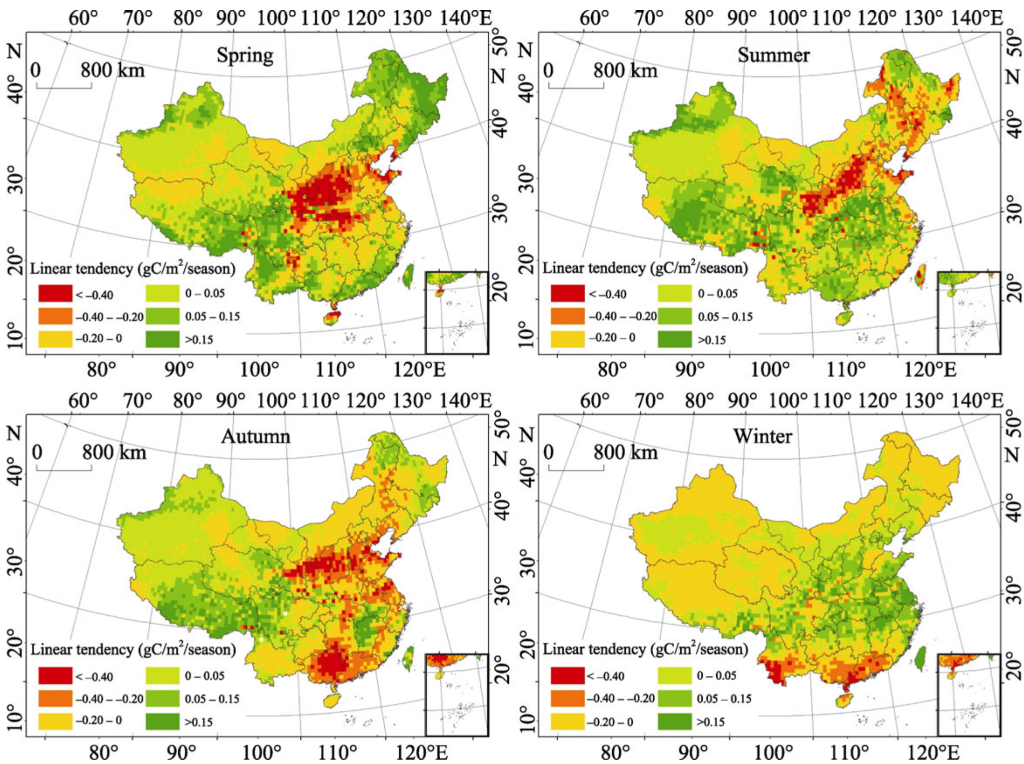

Figure 9 Seasonal NPP linear trends from 1961 to 2005

exceeding 0.40 gC/m^2/season. NPP in the provinces of Guangdong and Guangxi decreased drastically in autumn and winter but presented an upward trend in spring and summer. NPP in most parts of the Tibetan Plateau increased in spring, summer, and autumn. NPP in the Tianshan and Altay mountain areas increased slightly in spring, summer, and autumn and decreased slightly in winter. NPP increased significantly in spring in northeastern China. Regional differences in the increase or decrease of NPP were significant in summer and autumn.

4 Discussion

4.1 Relations between NPP variation and climate change

NPP exhibited climate-related zonality as demonstrated by the longitudinal and latitudinal NPP analyses (Figure 4). NPP decreased from south to north along with a decline in temperature and decreased from east to west with a reduction in precipitation. Thus, temperature and precipitation may be the main climate factors that affect NPP distribution and variation. The spatial distribution of China's terrestrial NPP shows that NPP was high in hot and moist areas. The tropics and subtropics have a temperate and moist climate, which is fit for the growth of almost all kinds of vegetation. NPP was greater than 900 gC/m^2/yr in areas where the dominant vegetation type is broadleaf evergreen forest. Climate conditions are relatively poor in eastern temperate areas, where NPP was generally within 300 gC/m^2/yr and 700 gC/m^2/yr. Broadleaf cold-deciduous forests are abundant in these areas. NPP in the Qinling−Dabashan and Changbai mountain areas was within the interval of 500 gC/m^2/yr to 700 gC/m^2/yr because of good moisture conditions. NPP in Inner Mongolia and central–eastern Tibet was generally between 100 gC/m^2/yr and 300 gC/m^2/yr because of the harsh climate. The main vegetation types in these regions are temperate steppe or alpine meadow and steppe. Little vegetation growth exists in the alpine and temperate desert areas of western Tibet and northwestern China. NPP was generally less than 30 gC/m$^{2/}$yr because of minimal precipitation or very low temperature. The Altay and Tianshan mountain areas had slightly better climate conditions, with grasses sparsely distributed. NPP was within the range of 30 gC/m^2/yr and 100 gC/m^2/yr.

Increase in temperature is important for the production of alpine ecosystems. For most tropical, subtropical, warm–temperate, and temperate areas, warm temperature may increase moisture evaporation and inhibit the production of the ecosystem (Figure 10b). Increase in NPP in the Greater Hinggan Mountains (Figure 8) may have been caused by the increase in temperature in the past decades (Figure 10a), especially in spring (Figure 9). The increasing trend of NPP (Figure 8) in the western Tibetan Plateau may be due to significant warming (Figure 10a).

Increased rainfall in most parts of China is beneficial to ecosystem production, especially in extremely arid desert regions. Increase in precipitation plays a key role in promoting ecosystem productivity (Figure 11b). The decrease in NPP in the past 45 years in Xishuangbanna (Figure 8) may have been caused by precipitation reduction (Figure 11a), especially in winter (Figure 9). The declining trend of NPP in the Loess Plateau (Figure 8) may have been caused by reduction in precipitation (Figure 11a).

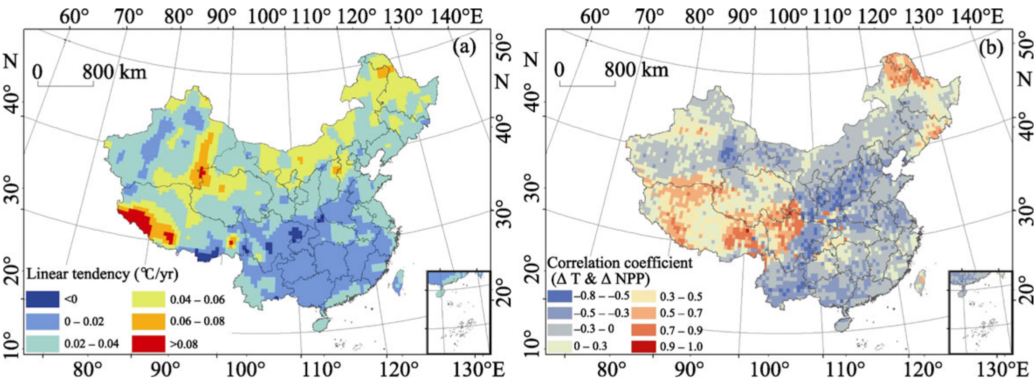

Figure 10 Temperature trend and correlation between NPP and temperature change

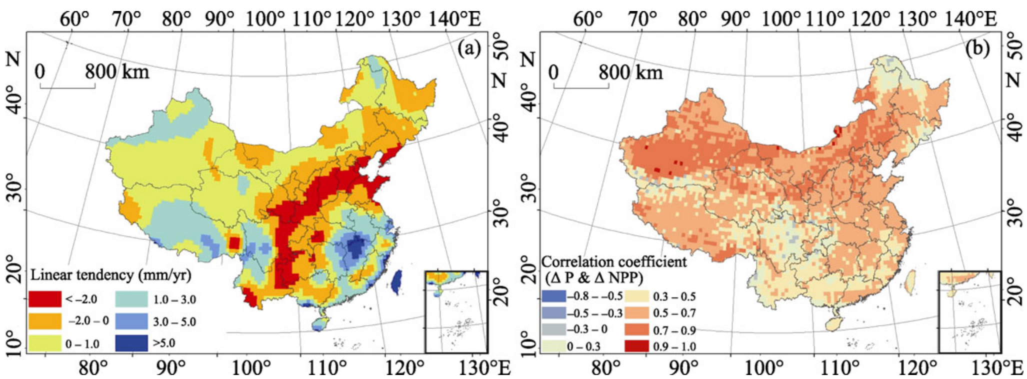

Figure 11 Precipitation trend and correlation between NPP and precipitation change

Climate change has greatly influenced the production of China's terrestrial ecosystem. This influence would be intensified by warm climate, frequent extreme weather events, and expanded regional disparities in precipitation in the future (Ding *et al*., 2006). In order to assess the influence and then take appropriate measures to adapt the climate change, research will focus on revealing the terrestrial ecosystem vulnerability to climate change in China, and identifying the potential leading factors of regional ecosystem vulnerability to climate change in the future.

4.2 Uncertainty analysis

4.2.1 Uncertainty in model verification

The lower limit of the simulated subtropical evergreen broadleaf forest was found to be lower than the measured range because of the low NPP simulation value for evergreen broadleaf forests in the valley of eastern Himalaya (generally ranging between 130 gC/m^2/yr and 600 gC/m^2/yr). This result may be attributed to the relatively low simulation accuracy (0.5°×0.5°) and the fact that the simulation results can only reflect the average performance of vegetation NPP within the latitude–longitude grids and not vegetation differences caused by small-scale changes in topography (the distribution of evergreen broadleaf trees in the valley area is generally from 1000 m to 1100 m). Simulation accuracy could be improved in the future to reduce uncertainty in vegetation simulation in complex terrains.

4.2.2 Uncertainty in NPP simulation

The total annual NPP simulated in this study was slightly higher than that in other relevant simulations (Table 3) probably because the simulation conducted in this research merely simulated the NPP dynamics of a potential natural ecosystem to study the response of China's terrestrial ecosystem to climate change. However, the influence of human activities on the terrestrial ecosystem is huge, especially with the rapid industrialization that occurred in the past several decades. A more comprehensive model should be designed to further understand the relationship of ecosystems, climate change, and human activities. By simulating the dynamics of terrestrial ecosystems based on land use and climate change, we can forecast the change in ecosystems in future studies and discuss the extent to which ecosystems could be changed.

5 Conclusions

This study verified the applicability of IBIS in the simulation of NPP in China's terrestrial ecosystems based on observed climatic, topographic, and soil data. The corresponding temporal and spatial variations in NPP in the past 45 years (1961 to 2005) were analyzed. The main conclusions are summarized below.

(1) The model-simulated NPP in this study can accurately reflect the overall pattern of terrestrial NPP in China, with the value within the relevant statistical parameters measured and close to the remote sensing estimation. IBIS can be utilized in the large-scale simulation of NPP in China's natural ecosystems and can be employed to study the dynamic interactions that occur between terrestrial ecosystems and climate change.

(2) The total NPP of China's terrestrial ecosystems under climate change in the past 45 years varied from 3.61 GtC/yr to 4.24 GtC/yr, with an average of 3.87 GtC/yr. Total NPP exhibited minimal increase or decrease in general. Regional differences in terms of NPP increase or decrease were significant but exhibited an insignificant overall linear trend. NPP declined in most parts of eastern and central China, especially in the Loess Plateau. NPP increased in most parts of western China, especially in the Kunlun Mountain areas, indicating that climate changes over the past 45 years conduct the natural ecosystem in this area toward an expecting direction.

(3) Total NPP in summer was generally higher than that in spring and autumn; total NPP in winter was the lowest. Similar to the fluctuation law of annual NPP, seasonal NPP also showed an insignificant increase or decline; the trend line was general level. The regional differences in seasonal NPP change were significant. NPP decreased in spring, summer, and autumn in most parts of the Loess Plateau but increased in most parts of the Tibetan Plateau.

Acknowledgements

Meteorological observation data was obtained from China Meteorological Data Sharing Service System, and the Chinese digital elevation model (DEM) was provided by the Data Sharing Infrastructure of Earth System Science of China. The IBIS code and soil data were derived from the Center for Sustainability and the Global Environment (SAGE).

References

Cao Mingkui, Tao Bo, Li Kerang *et al*., 2003. Interannual variation in terrestrial ecosystem carbon fluxes in China from 1981 to 1998. *Acta Botanica Sinica*, 45(5): 552–560. (in Chinese)

Delire C, Foley J A, 1999. Evaluating the performance of a land surface/ecosystem model with biophysical measurements from contrasting environments. *Journal of Geophysical Research–Atmospheres*, 104(D14): 16895–16909.

Ding Yihui, Ren Guoyu, Shi Guangyu *et al*., 2006. National assessment report of climate change (I): Climate change in China and its future trend. *Advances in Climate Change Research*, 2(1): 3–8. (in Chinese)

El Maayar M, Price D, Delire T C *et al*., 2001. Validation of the integrated biosphere simulator over Canadian deciduous and coniferous boreal forest stands. *Journal of Geophysical Research–Atmospheres*, 106(D13): 14339–14355.

El Maayar M, Price D T, Black T A *et al*., 2002. Sensitivity tests of the integrated biosphere simulator to soil and vegetation characteristics in a pacific coastal coniferous forest. *Atmosphere–Ocean*, 40(3): 313–332.

Field C B, Behrenfeld M J, Randerson J T *et al*., 1998. Primary production of the biosphere: Integrating terrestrial and oceanic components. *Science*, 281(5374): 237 – 240.

Foley J A, Levis S, Prentice I C *et al*., 1998. Coupling dynamic models of climate and vegetation. *Global Change Biology*, 4(5): 561–579.

Foley J A, Prentice I C, Ramankutty N *et al*., 1996. An integrated biosphere model of land surface processes, terrestrial carbon balance, and vegetation dynamics. *Global Biogeochemical Cycles*, 10(4): 603–628.

Friend A D, Stevens A K, Knox R G *et al*., 1997. A process-based terrestrial biosphere model of ecosystem dynamics (Hy–brid v3.0). *Ecological Modelling*, 95(2/3): 249–287.

Fu Bojie, Niu Dong, Zhao Shidong, 2005. Study on global change and terrestrial ecosystems: History and prospect. *Advance in Earth Sciences*, 20(5): 556–560. (in Chinese)

Gao Zhiqiang, Liu Jiyuan, Cao Mingkui, 2004. Impacts of land use and climate change on regional net primary productivity. *Journal of Geographical Sciences*, 14(3): 581–591.

Haxeltine A, Prentice I C, 1996. BIOME3: An equilibrium terrestrial biosphere model based on eco-physiological constraints and competition among plant functional types. *Global Biogeochemical Cycles*, 4(10): 693–708.

Huang Mei, 2006. Study of the water, energy and carbon fluxes of China's terrestrial ecosystems. Beijing: Ph.D Dissertation of Institute of Geographic Sciences and Natural Resources Research, CAS. (in Chinese)

Hutchinson M F, 2004. Anusplin version 4.3 user guide. The Australia National University, Center for Resource and Environment Studies, Canberra.

IPCC, 2007. Climate Change 2007: The Physical Science Basis: Contribution of Working Group I to the Fourth Assessment Report of the Intergovernmental Panel on Climate Change. Cambridge: Cambridge University Press.

Kucharik C J, Barford C C, El Maayar M *et al*., 2006. A multiyear evaluation of a dynamic global vegetation model at three AmeriFlux forest sites: Vegetation structure, phenology, soil temperature, and CO_2 and H_2O vapor exchange. *Ecological Modelling*, 196(1/2): 1–31.

Kucharik C J, Foley J A, Delire C *et al*., 2000. Testing the performance of a dynamic global ecosystem model: Water balance, carbon balance, and vegetation structure. *Global Biogeochemical Cycles*, 14(3):795–825.

Lieth H, Whittaker R H, 1975. Primary Productivity of the Biosphere. Berlin: Springer.

Liu J X, Price D T, Chen J A, 2005. Nitrogen controls on ecosystem carbon sequestration: A model implementation and application to Saskatchewan, Canada. *Ecological Modelling*, 186: 178–195.

Liu Shirong, Wu Deying, Wang Bing *et al*., 1993. Impacts of climate change on productivity of forests in China. *Forest Research*, 6(6): 633–642. (in Chinese)

Liu Zhiang, Ma Qinyan, Pan Xiangli, 1994. Study of the biomass and productivity of natural Larix gmelini. *Acta Phytoecologica Sinica*, 18(4): 328–337.

Matthew P A, Lombardero M J, 2000. Assessing the consequences of global change for forest disturbance from herbivores and pathogens. *Science of the Total Environment*, (262): 263–286.

Naik V, Wuebbles D J, DeLucia E H *et al*., 2003. Influence of geoengineered climate on the terrestrial biosphere.

Environmental Management, 32(3): 373–381.

Ni J, 2000. Net primary production, carbon storage and climate change in Chinese biomes. *Nordic Journal of Botany*, 20(4): 415–426.

Parry M L, Canziani O F, Palutikof J P *et al*., 2007. Climate Change 2007: Impacts, adaptation and vulnerability: Contribution of Working Group II to the Fourth Assessment Report of the Intergovernmental Panel on Climate Change. Cambridge: Cambridge University Press.

Parton W J, Scurlock J M O, Ojima D S, 1993. Observations and modeling of biomass and soil organic matter dynamics for grassland biome worldwide. *Global Biogeochemical Cycles*, 7(4): 785–809.

Piao S L, Fang J Y, 2003. Seasonal changes in vegetation activity in response to climate changes in China between 1982 and 1999. *Acta Geographica Sinica*, 58(1): 119–125. (in Chinese)

Prentice I C, Cramer W, Harrison S P *et al*., 1992. A global biome model based on plant physiology and dominance, soil properties and climate. *Journal of Biogeography*, 19(2): 117–134.

Ruimy A, Saugier B, Dedieu G, 1994. Methodology for the estimation of terrestrial net primary production from remotely sensed data. *Journal of Geophysical Research*, 99(D3): 5263–5283.

Running S W, Gower S T, 1991. Forest-BGC, a general model of forest ecosystem processes for regional applications (II): Dynamic allocation and nitrogen budgets. *Tree Pbysiol*., 9: 147–160

Sitch S, Prentice I C, Smith B, 2000. LPJ: a coupled model of vegetation dynamics and the terrestrial carbon cycle. In: Sitch S (ed.). The role of vegetation dynamics in the control of atmospheric CO_2 content. Lund: Ph.D Dissertation of Lund University.

Sun Rui, Zhu Qijiang, 2001. Effect of climate change of terrestrial net primary productivity in China. *Journal of Remote Sensing*, 5(1): 58–61. (in Chinese)

Tao Bo, Li Kerang, Shao Xuemei *et al*., 2003. The temporal and spatial patterns of terrestrial net primary productivity in China. *Journal of Geographical Sciences*, 13(2): 163–171.

Twine T E, Kucharik C J, Foley J A, 2004. Effects of land cover change on the energy and water balance of the Mississippi River basin. *Journal of Hydrometeorology*, 5(4): 640–655.

Vano J A, Foley J A, Kucharik C J *et al*., 2006. Evaluating the seasonal and interannual variations in water balance in northern Wisconsin using a land surface model. *Journal of Geophysical Research–Biogeosciences*, 111, doi: 10.1029/2005JG000112.

Wang Yuhui, Zhou Guangsheng, Jiang Yanling *et al*., 2001. Estimating biomass and NPP of Larix forests using forest inventory data. *Acta Phytoecologica Sinica*, 25(4): 420–425. (in Chinese)

Wang Zongming, Liang Yinli, 2002. Progress in vegetation net primary productivity model research. *Journal of Northwest Forestry College*, 17(2): 22–25. (in Chinese)

Wu Shaohong, Dai Erfu, Huang Mei *et al*., 2007. Ecosystem vulnerability of China under B2 climate scenario in the 21st century. *Chinese Science Bulletin*, 52(10): 1379–1386. (in Chinese)

Wu Shaohong, Zheng Du, Yin Yunhe *et al*., 2010. Northward-shift of temperature zones in China's eco-geographical study under future climate scenario. *Journal of Geographical Sciences*, 5(5): 643–665.

Xiao X M, Melillo J M, Kicklighter D W *et al*., 1998. Net primary production of terrestrial ecosystems in China and its equilibrium responses to changes in climate and atmospheric CO_2 concentration. *Acta Phytoecologica Sinica*, 22(2): 97–118.

Yuan Q Z, Zhao D S, Wu S H *et al*., 2011. Validation of the integrated biosphere simulator in simulating the potential natural vegetation map of China. *Ecological Research*, 26(5): 917–929

Zhao Dongsheng, 2010. Possible impacts of future climate change to natural ecosystems productivity in China. Beijing: Postdoctor Report of Institute of Geographical Sciences and Natural Resource Research, CAS. (in Chinese)

Zhao Ming, Zhou Guangsheng, 2005. Modeling Variation Trend of Boreal Forest NPP in China and Its Relations to Temperature and Precipitation. *Acta Botanica Boreali–Occidentalia Sinica*, 25(3): 466–471. (in Chinese)

Zheng Z, Wang G, 2007. Modeling the dynamic root water uptake and its hydrological impact at the Reserva Jaru site in Amazonia. *Journal of Geophysical Research–Biogeosciences*, 112, doi: 10.1029/2007JG000413.

Zhu Q A, Jiang H, Liu J X *et al*., 2010. Evaluating the spatiotemporal variations of water budget across China over 1951–2006 using IBIS model. *Hydrological Processes*, 24(4): 429–445.